Dynamical response and switching of an optically bistable anharmonic oscillator

Burke Ritchie* and Charles M. Bowden
Research Directorate, Research, Development, and Engineering Center, U.S. Army Missile Command, Redstone Arsenal, Alabama 35898-5248
(Received 3 December 1984)

The dynamical solution of the driven classical anharmonic (AH) oscillator is obtained through a region of optical bistability. The dynamical solution is observed to switch from the lowest to highest steady-state (SS) root near a SS turning point with evidence of critical slowing down. The solution of a widely used multiple-photon version of the AH model is also obtained and is found to give qualitatively similar behavior. The average number of photons observed dramatically increases in the bistable region and exhibits damped oscillations.

I. INTRODUCTION

Optical bistability (OB) is currently a very active research area in nonlinear optics.[1] Certain authors[2–5] have emphasized that under certain conditions optical bistability is an intrinsic property of a nonlinear material itself (i.e., without resonator or cavity feedback). Indeed, this is most easily seen in recent studies[2,3] on the classical Duffing oscillator, whose steady-state (SS) solution for the oscillator amplitudes shows mirrorless optical bistability (MOB), in a region of its parameter space. Thus, for a single value of an input field, there can exist an intrinsic bistable response of the system. The MOB is due entirely to what amounts to an excitation-dependent frequency shift caused by the anharmonic contribution and, of course, the excitation is driven by the oscillator-field interaction. In view of the importance of this effect in such areas as molecular multiple-photon absorption[6,7] and nonlinear response of a field mode to a nonlinear dispersive medium,[8] it appears very worthwhile to generate the exact numerical dynamical solution for the classical anharmonic oscillator to study the dynamics of switching and the stability of the SS predictions. The dynamical solution of an often used[6–8] multiple-photon anharmonic model is also generated for comparison.

The model for the driven, damped Duffing oscillator is presented in the next section and the steady-state and dynamical solutions are developed using a well-known modal expansion. The equations of motion for a widely used multiple-photon counterpart to the classical Duffing oscillator are presented in Sec. III and the dynamical evolution and stability analysis are presented for comparison with the results of Sec. II. The dynamical evolution and the method for calculating the expectation value for the number of photons absorbed are presented in Sec. IV and the results for the two cases are compared and discussed.

TABLE I. Parameters used in the numerical calculations.

$\omega_0=10^{14}\ \mathrm{s}^{-1}$	$\mu=10^{-23}\ \mathrm{g}$
$\gamma_d=10^{11}\ \mathrm{s}^{-1}$	$d'=10^{-10}\ \mathrm{erg}^{1/2}\,\mathrm{cm}^{1/2}$
$\gamma_1=3\times10^{35}\ \mathrm{s}^{-2}\,\mathrm{cm}^{-1}$	$\epsilon_0=10.5\times10^{6}\ \mathrm{V\,cm}^{-1}$

The results of the calculations are summarized and discussed in Sec. V and Sec. VI is used for conclusion.

II. DYNAMICS OF BISTABILITY IN THE DUFFING OSCILLATOR

The classical equation of motion for the anharmonic oscillator (in which terms in the potential through cubic are retained) is

$$\ddot{q}+\gamma_d\dot{q}+\omega_0^2 q-\gamma_1 q^2=\frac{f(t)}{\mu}\cos(\omega t)\ , \tag{1}$$

where γ_d is a damping rate due to an assumed coupling[3] with other oscillator modes, μ is the oscillator reduced mass, and ω_0 and γ_1 are defined from the expansion of the potential

$$V\simeq V(R_e)+\tfrac{1}{2}\mu\omega_0^2 q^2-\tfrac{1}{3}\mu\gamma_1 q^3+\cdots \tag{2}$$

about the position R_e of its minimum. The driving force $f(t)$ is defined as $d'\epsilon(t)$, where d' is the slope of the oscillator permanent dipole moment at R_e and $\epsilon(t)$ is the slowly varying part of the laser field strength [taken here to be $\epsilon_0 t/\tau_p$ or $\epsilon_0(2\tau_p-t)/\tau_p$ for $t<\tau_p$ or $t>\tau_p$, respectively, where ϵ_0 is a peak field strength and τ_p is a pulse half-width]. Physically realistic values of these parameters are given in Table I.

In the same way as in the analysis of Flytzanis and Tang[3] (FT), we seek a solution by expanding q,

$$q=\tfrac{1}{2}(q_0+q_{+1}e^{i\omega t}+q_{-1}e^{-i\omega t}+\cdots)\ , \tag{3}$$

and equating coefficients of $e^{\pm i\omega t}$. This leads to the set of coupled, nonlinear differential equations,

$$\ddot{q}_0+\gamma_d\dot{q}_0+\omega_0^2 q_0-\tfrac{1}{2}\gamma_1 q_0^2-\gamma_1 q_{+1}q_{-1}=0\ , \tag{4a}$$

$$\ddot{q}_{\pm1}\pm2i\omega\dot{q}_{\pm1}+\gamma_d\dot{q}_{\pm1}\pm i\omega\gamma_d q_{\pm1}+(\omega_0^2-\omega^2)q_{\pm1}-\gamma_1 q_0 q_{\pm1}=\frac{f(t)}{\mu}\ . \tag{4b}$$

The SS solution is obtained by setting the time derivatives in Eqs. (4) equal to zero. Then,

$$q_{+1}^{(SS)}=\frac{f(t)/\mu}{\Delta^2\pm i\omega\gamma_d-(\gamma_1/\omega_0)^2 q_{+1}^{(SS)}q_{-1}^{(SS)}}\ , \tag{5a}$$

$$\Delta^2=\omega_0^2-\omega^2\ , \tag{5b}$$

where for $\gamma_1/\omega_0^2 \ll 10^8$ cm^1, $q_0^{(SS)}\simeq(\gamma_1/\omega_0^2)q_{+1}^{(SS)}q_{-1}^{(SS)}$.

Following Flytzanis and Tang,[3] it is convenient to find the roots of the equation for $q_{+1}^{(SS)}q_{-1}^{(SS)}=|q_{+1}^{(SS)}|^2$. Then $|q_{+1}^{(SS)}|$ (r in FT's work) is $\sqrt{2}$ times the root-mean-square (rms) solution (in SS) implied by the first-order part of Eq. (3). [FT's detuning is $-\Delta$, and their anharmonicity constant has a different meaning from ours in that our $-\gamma_1 q^2$ in Eq. (1) is replaced by γq^3 as appropriate for the Duffing oscillator. A consequence of this difference is that the optically bistable region occurs for $\pm\Delta$ herein and in FT, respectively.] The SS problem reduces to finding the roots of the cubic equation

$$x^3+ax+b=0\ , \tag{6a}$$

$$|q_{+1}^{(SS)}|^2=x+\frac{2}{3}\left[\frac{\Delta\omega_0}{\gamma_1}\right]^2\ , \tag{6b}$$

$$a=\left[\frac{\omega_0}{\gamma_1}\right]^4[(\omega\gamma_d)^2-\tfrac{1}{3}\Delta^4]\ , \tag{6c}$$

$$b=\left[\frac{\omega_0}{\gamma_1}\right]^4\left\{\frac{2}{3}\left[\frac{\Delta\omega_0}{\gamma_1}\right]^2[(\omega\gamma_d)^2+\tfrac{1}{9}\Delta^4]-[f(t)/\mu]^2\right\}\ . \tag{6d}$$

Optical bistability occurs when Eq. (6a) has three real roots, which occurs when $b^2/4+a^3/27<0$. These roots are plotted in Fig. 1 where we use the time axis for convenience in comparing with the dynamical results. Note that a must be negative. Then $b^2/4<|a^3/27|$. Our experience shows that this occurs when the two terms in (6d) tend to cancel (which requires that $\Delta^2>0$). Thus, for small times, $f(t)/\mu$ in Eq. (6d) is too small for the condition to be satisfied, and we are in a single small-root region. Then we pass into the bistable region with increasing $f(t)/\mu$. Then we pass into the single large-root region for maximum strengths where $[f(t)/\mu]^2$ becomes too large for the condition to be satisfied. The solution is symmetric on either side of $\tau_p=100$ ps. The dynamical solution is also obtained by direct numerical integration of Eqs. (4).

III. DYNAMICS OF BISTABILITY IN THE ANHARMONIC MULTIPLE-PHONON TRANSITION MODEL

For comparison, the Heisenberg equations for the expectation values A and N of the shift and number operators, a and $a^\dagger a$, respectively, for a widely used quantized anharmonic oscillator model[6–8] are solved numerically. In the rotating-wave approximation (RWA), the equations for $A=\langle a\rangle$ and $N=\langle a^\dagger a\rangle$ are[6]

$$\dot{A}=-i\delta A-\tfrac{1}{2}\gamma_d A+2i\chi NA-\frac{i}{2}\Omega\ , \tag{7a}$$

$$\dot{N}=\frac{i}{2}\Omega(A-A^*)-\gamma_d N\ , \tag{7b}$$

where

$$\chi=\frac{5}{12}\frac{\hbar\gamma_1^2}{\mu\omega_0^4},\quad \Omega=\frac{d'\epsilon(t)}{\sqrt{2\mu\hbar\omega_0}} \tag{7c}$$

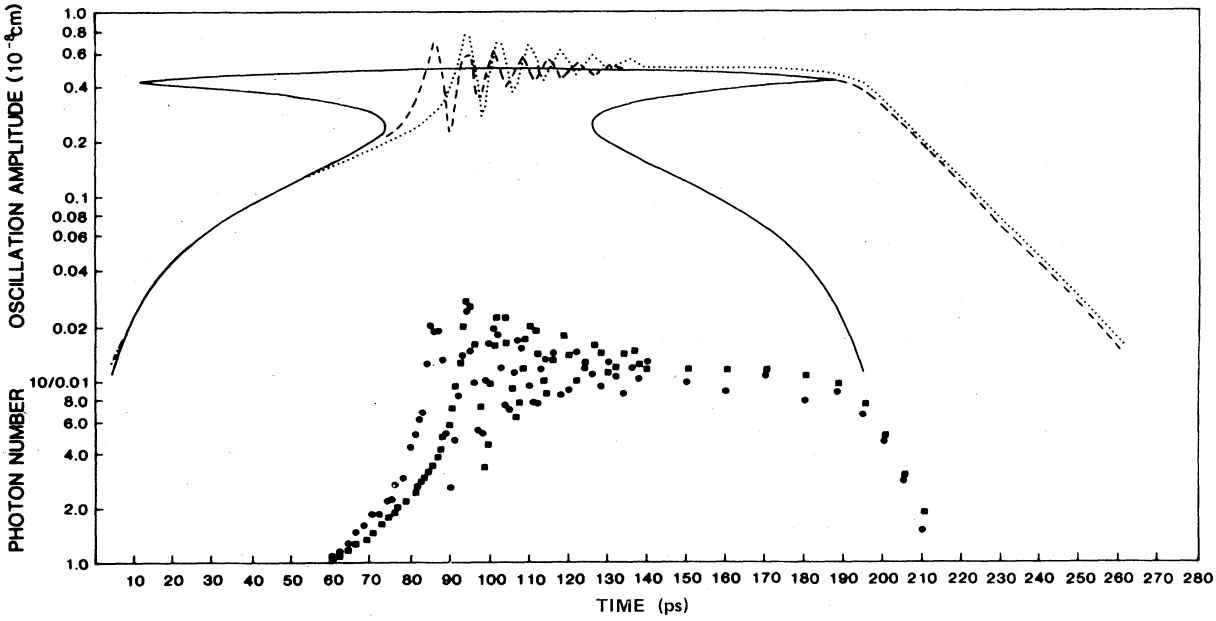

FIG. 1. Results for $\delta=\omega_0-\omega=0.8\times10^{12}$ s^{-1} and the parameters of Table I. Solid curve: classical steady-state solution; dashed curve: classical dynamical solution; dotted curve: multiple-photon dynamical solution; dots: classical dynamical solution; squares: multiple-photon dynamical solution.

and $\delta=\omega_0-\omega$. It should be pointed out that Eqs. (7a) and (7b) are based upon an approximate Hamiltonian[6] with regard to the cube of the operator q and that low-order decorrelation is required to close the hierarchy of equations to Eqs. (7a) and (7b). It is further noted that Eqs. (7a) and (7b) are the continuum limit for the quasicontinuum coupling treated in Ref. 7, which leads to relaxation and damping (Ref. 9), γ_d. In lowest-order decorrelation, Eq. (7b) can be obtained directly from Eq. (7a).

The steady-state solution of Eqs. (7) results in the equation of state,

$$\Omega^2=4N[\tfrac{1}{4}\gamma_d^2+(\delta-2\chi N)^2]\,, \tag{8}$$

which is identical in form to the corresponding SS solution obtained from Eq. (6a) and that discussed by Flytzanis and Tang.[3] The condition for OB, i.e., two real positive roots for N for a given driving field Ω, is that $\delta/\gamma_d>\frac{1}{2}\sqrt{3}$. For the condition $\delta^2/\gamma_d^2\gg 1$, the high-field (Ω_h) and low-field (Ω_l) switching points are $\Omega_h=\frac{2}{27}\delta^3/\chi$ and $\Omega_l=\frac{1}{8}\delta\gamma_d^2/\chi$. Using the relations, Eqs. (7c), and the correspondence

$$|q_+|=\left[\frac{2\hbar}{\mu\omega_0}\right]^{1/2}|A|\,,\quad \left[\hat{q}=\left[\frac{\hbar}{2\mu\omega_0}\right]^{1/2}(ae^{-i\omega t}+a^\dagger e^{i\omega t})\right]\,,$$

Ω_h and Ω_l are each $\frac{6}{5}$ of the corresponding values obtained from the equation of state[3] from Eq. (5a).

In Fig. 1 we plot $|q_+|$ [both the dynamical and SS solutions from Eqs. (4) and (5), respectively] and $(2\hbar/\mu\omega_0)^{1/2}|A|$ [the dynamical solution from Eq. (7a)]. Note that both of these quantities correspond physically to $\sqrt{2}$ times the root-mean-square (rms) values of the oscillator position which would be obtained if one treated the slowly varying parts of the solution (q_+, q_-, $\langle a^\dagger\rangle$, and $\langle a\rangle$) as constant relative to the rapidly varying parts. For example,

$$\sqrt{2}\langle\hat{q}\rangle_{\rm rms}\simeq\left[\frac{2\hbar}{\mu\omega_0}\right]^{1/2}\langle a^\dagger\rangle\langle a\rangle=\left[\frac{2\hbar}{\mu\omega_0}\right]^{1/2}|A|\,.$$

Similarly $\sqrt{2}\langle q-\frac{1}{2}q_0\rangle_{\rm rms}\simeq|q_+|$, where q is the classical oscillator position [Eqs. (1) and (3)].

A linear stability analysis[10] yields the eigenvalues

$$\lambda_\pm=-\tfrac{1}{2}\gamma_d\pm i(\delta^2+12\chi^2N^2-8\chi N\delta)^{1/2}\,, \tag{9}$$

from which a solution representing a small displacement from the SS solution can be constructed as a linear combination of exponentials whose arguments are $\lambda_\pm t$. Points lying on the equation of state [Eq. (8)] are stable or unstable depending on whether $\mathrm{Re}\lambda_\pm<0$ or $\mathrm{Re}\lambda_\pm>0$, respectively. It is easily verified from (8) and (9) that all points on the SS curve in Fig. 1 between the turning points and the upper and lower roots are unstable, whereas all other points are stable. Damped oscillations (Fig. 1 above about 80 ps) occur for displacements from the SS solution when the term in the square root is positive. Instabilities occur when it is negative and the second term of Eq. (9) is greater than $\frac{1}{2}\gamma_d$. Equation (9) is evaluated for $\delta=0.8\times10^{12}$ s^{-1}, $\chi=3.95\times10^{10}$ s^{-1} [Eq. (7c)], and $N=\langle a^\dagger a\rangle\simeq\langle a^\dagger\rangle\langle a\rangle=|A|^2\simeq11.9$. The latter quantity is estimated graphically (Fig. 1) from the SS classical value of $|q_+^{(\rm SS)}|$ and the correspondence $|q_+|=(2\hbar/\mu\omega_0)^{1/2}|A|\simeq0.5\times10^{-8}$ cm (near 100 ps). The second term in Eq. (9) is calculated to be $\pm i(0.53\times10^{12}$ s$^{-1})$. From Fig. 1 a graphical determination of the oscillation frequency (near 100 ps) gives a value of $\pm i(0.78\times10^{12}$ s$^{-1})$, which is very nearly the value for the detuning δ. The agreement is reasonable given that N is determined from the classical SS solution.

Even though the SS, Eq. (8) is identical in form with the relation obtained using conditions given by Eqs. (6), the turning points differ slightly due to small discrepancies in the numerical parameters according to Eqs. (7c). It is not at all clear that the dynamical evolution for the two models should show close similarity. There are in general two coupled first-order equations in real variables which correspond to Eq. (7a), and because of the anharmonic contribution, these cannot be precisely reduced to a single second-order equation, even in the absence of damping γ_d. Equation (7b) can be obtained from Eq. (7a) using the relation $N=|A|^2$. Since $N=\langle a^\dagger a\rangle$, and $N\simeq\langle a^\dagger\rangle\langle a\rangle=|A|^2$ only if $a^\dagger$ and a are approximately decorrelated, the $N=|A|^2$ result suggests that the model described by Eqs. (7) (based on the transformed Hamiltonian of Narducci *et al.*[6]) is essentially classical in character and not a true test of quantum mechanical (QM) effects in the anharmonic oscillator. The close numerical agreement of the results of the two models (Fig. 1) reinforces this observation. This is entirely consistent with the results of Rozanov and Smirnov[11] who considered the Schrödinger equation through the fourth-order anharmonic contribution and showed that the quantum effects in the hysteresis regime are unimportant if the oscillation amplitude sufficiently exceeds the width of the wave packet.

IV. DYNAMICAL EVOLUTION AND PHOTON STATISTICS

In Fig. 1 the dynamical results from integration of Eqs. (4b) and (7a) for the magnitude of the oscillator amplitudes are plotted versus time for comparison. The time axis represents a ramping field. Superposed is the SS relation from conditions given by Eqs. (6) with the SS field corresponding to the instantaneous value of the ramping field as indicated on the horizontal axis. Also plotted is the expectation value of the number of photons absorbed versus time for the two cases. The latter is determined by time integration of Eq. (7b) for the model based upon quantization of the anharmonic oscillator[6] (QM) model;

for the classical anharmonic oscillator, it is given approximately by

$$\langle n \rangle \simeq \sum_{n=0}^{\infty} nP_n = \epsilon_0 , \tag{10a}$$

$$P_n = \frac{e^{-\epsilon_0}}{n!}\epsilon_0^n , \tag{10b}$$

$$\epsilon_0 = \tfrac{1}{2}\mu \frac{(\dot{q}^2 + \omega_0^2 q^2)}{\hbar\omega_0} . \tag{10c}$$

The Poisson distribution (for the probability of populating the nth level from $n=0$ at $t=0$) is the exact result[12] for a harmonic oscillator forced by a term linear in q. For the harmonic case q is given by Eq. (1) with $\gamma_d = \gamma_1 = 0$ and is observed to diverge with t for $\omega = \omega_0$. For an oscillator which is damped ($\gamma_d \neq 0$) and/or anharmonic ($\gamma_1 \neq 0$), q is, of course, finite on resonance ($\omega = \omega_0$), and the average number of photons absorbed ϵ_0 [Eq. (10a)] is just the ratio of the classical oscillator energy at any time to the energy of one vibrational quantum. Finite damping and anharmonicity, which are crucial to a physically sensible solution of Eq. (1), also appear in the Schrödinger equation[12] for the oscillator. However, if these are treated as small perturbations there, then in zeroth order, Eqs. (10) hold, with q calculated from Eq. (1).

V. DISCUSSION

One obvious effect of neglecting anharmonic terms in the Schrödinger equation [while including them in Eq. (1)] is the neglect of unequal level spacing in Eqs. (10). However, the qualitative agreement between $\langle n \rangle$ and N [from Eq. (7b)] suggests that Eq. (10c) is a reasonable estimate of the average number of photons absorbed, at least within the limitations of both theories. In Fig. 1 (and in other calculations not presented here), $\langle n \rangle$ and N [from Eq. (7b)] agree almost quantitatively in the optically nonbistable region of the motion and qualitatively in the bistable region. In the optically bistable region, where the dynamical $|q_{\pm 1}|$ switches from $|q_{\pm 1}^{(SS)}|$ (lower root) to $|q_{\pm 1}^{(SS)}|$ (higher root), the character of the absorption is dramatically altered. The magnitude of the oscillator amplitude as calculated from Eqs. (7) is observed to follow the lower SS root of the classical equation up to the switching region where it evolves more slowly to the upper state compared to the classical result. As the field is ramped down past the lower critical field, both solutions relax toward the lower SS by exponential decay governed by the relaxation rate γ_d. The switching-up time (i.e., the time of transit from the lower state to the first crossing of the upper state) for the classical anharmonic oscillator (AHO) is $\tau_c \simeq 9.73$ ps, whereas that for the multiple photon AHO is $\tau_Q \simeq 12.5$ ps.

The switch-up rate is governed in both cases by a combination of contributing factors. The critical slowing down in the neighborhood of the switching point as determined from Eq. (9) extends the rise time beyond a Rabi half-period, and this is expected to become more evident the slower the ramping rate of the field. The rise times are noticeably different in the two cases and, since the conditions are identical, this is a manifestation of discrepancy in dynamical response in the neighborhood of the region of critical slowing down.

The increased absorption in the bistable region is significant, especially since bistability occurs under nonresonant conditions. Indeed the detuning δ is here 0.8×10^{12} s^{-1} or over 30% of the Rabi rate [Eqs. (7c)] at its peak value (at 100 ps). For this detuning, the absorption by a nonbistable oscillator is minimal; for example, see Fig. 1 for times less than the onset of the bistable behavior (i.e., less than about 60 ps). Also, other calculations at $\delta = 0.9\times10^{12}$ s^{-1}, where no dynamical switch occurs since Δ^2 [see Eqs. (6)] is too large relative to the field strength for the upper critical point to be approached, show that the maximum number of photons absorbed is less than about 1.5.

VI. CONCLUSION

We have presented here the dynamical response of a Duffing oscillator in the bistable region, the steady-state properties of which were analyzed earlier by Flytzanis and Tang[3] (more recently by Goldstone and Garmire with propagation of the field included), and compared the behavior with that of a widely used[6–8] model based upon a quantized anharmonic oscillator. The results exhibit critical slowing down in the switching dynamics and stability in the bistable region. These results give impetus for further studies of cavityless optical bistability for systems corresponding to more physically realistic potential functions in order to eliminate the model dependence of the results. Also further study is required to reconcile the classical and multiple-photon model results by solving the quantum problem for the unapproximated model Hamiltonian without the requirements of lowest-order decorrelation.

ACKNOWLEDGMENTS

The authors would like to thank J. H. Eberly and J. W. Haus for their careful reading of the manuscript and for helpful comments and criticisms concerning it. One of us (B.R.) was partially supported by Battelle Columbus Laboratories, Contract No. DAAG29-81-D-0100.

---

*Permanent address: Chemistry Department, University of Alabama, University, Albama 35486.

[1]See, *Optical Bistability,* edited by C. M. Bowden, M. Ciftan, and H. R. Robl (Plenum, New York, 1981); *Optical Bistability 2,* edited by C. M. Bowden, H. M. Gibbs, and S. L. McCall (Plenum, New York, 1984).

[2]J. A. Goldstone and E. Garmire, Phys. Rev. Lett. 53, 910 (1984). This paper also contains a brief review of recent stud-

ies in "intrinsic" optical bistability.

[3]Chr. Flytzanis and C. L. Tang, Phys. Rev. Lett. **45**, 441 (1980).

[4]F. A. Hopf, C. M. Bowden, and W. H. Louisell, Phys. Rev. A **29**, 2591 (1984).

[5]C. M. Bowden and C. C. Sung, Phys. Rev. A **19**, 2393 (1979); C. M. Bowden, XI IQEC, IEEE Report, Catalogue No. 80CH1561-0, 1980, p. 589 (unpublished); C. M. Bowden, Ref. 1, p. 405.

[6]L. M. Narducci, S. S. Mitra, R. A. Shatas, and C. A. Coulter, Phys. Rev. A **16**, 247 (1977).

[7]J. R. Ackerhalt, H. W. Galbraith, and P. W. Milonni, Phys. Rev. Lett. **51**, 1259 (1983).

[8]P. D. Drummond and D. F. Walls, J. Phys. A **13**, 725 (1980).

[9]The authors of Ref. 7 appropriately consider coupling to a quantized discrete energy-level background; however, this causes the equations of motion, and the results, to be considerably more complicated. In the continuum limit, the background gives rise to damping and relaxation γ_d, and the resulting equations are (7a) and (7b).

[10]L. A. Lugiato, in *Progress in Optics XXI,* edited by E. Wolf (North-Holland, Amsterdam, 1984), p. 115.

[11]N. N. Rozanov and V. A. Smirnov, Pis'ma Zh. Eksp. Teor. Fiz. **33**, 504 (1981) [JETP Lett. **33**, 488 (1981)].

[12]E. Kerner, Can. J. Phys. **36**, 371 (1958). See also, R. J. Glauber, Phys. Rev. A **131**, 2766 (1963) in the context of the harmonic oscillator coherent-state representation.